N O T I C E

THIS DOCUMENT HAS BEEN REPRODUCED FROM
MICROFICHE. ALTHOUGH IT IS RECOGNIZED THAT
CERTAIN PORTIONS ARE ILLEGIBLE, IT IS BEING RELEASED
IN THE INTEREST OF MAKING AVAILABLE AS MUCH
INFORMATION AS POSSIBLE

CARSON ALEXIOU CORPORATION

NASA AMES INFRARED DETECTOR ASSEMBLIES

FINAL REPORT

NAS2- 10136

OCTOBER 15, 1979

NASA Ames Infrared Detector Assemblies Final Report

1.0   INTRODUCTION

The purpose of this contract was to design, fabricate, and test Si:Ga infrared detector assemblies using techniques representative of those used for hybrid arrays to determine the suitability of this candidate technology for infrared astronomical detector array applications. This final report will describe the design, fabrication methods, and test results of both the single channel assembly and the assembly using the Carson Alexiou Corporation 32-channel CMOS multiplexer.

2.0   DETECTOR MATERIAL

The detector material used for this effort was Si:Ga grown by Atomergic Chemicals Corporation and certified by them to have a boron background of less than 10^{13} atoms/cm^2 counter doped with phosphorus. The gallium concentration is 2×10^{16} atoms/cm^3. No further materials tests were made to characterize the detector material. Facilities are available with which to perform Hall vs. temperature measurements in the future for further characterization of detector material.

Detector resistance vs. temperature results were performed in May of 1979 and reported in that month's Progress Report. The detector resistance vs. temperature agreed approximately with theoretically predicted values. It was 200Ω at room temperature, reaching almost 1×10^{11} at 20-30°K as shown in Figure 1. These tests indicated approximately proper doping but did not prove that the detectors would necessarily work.
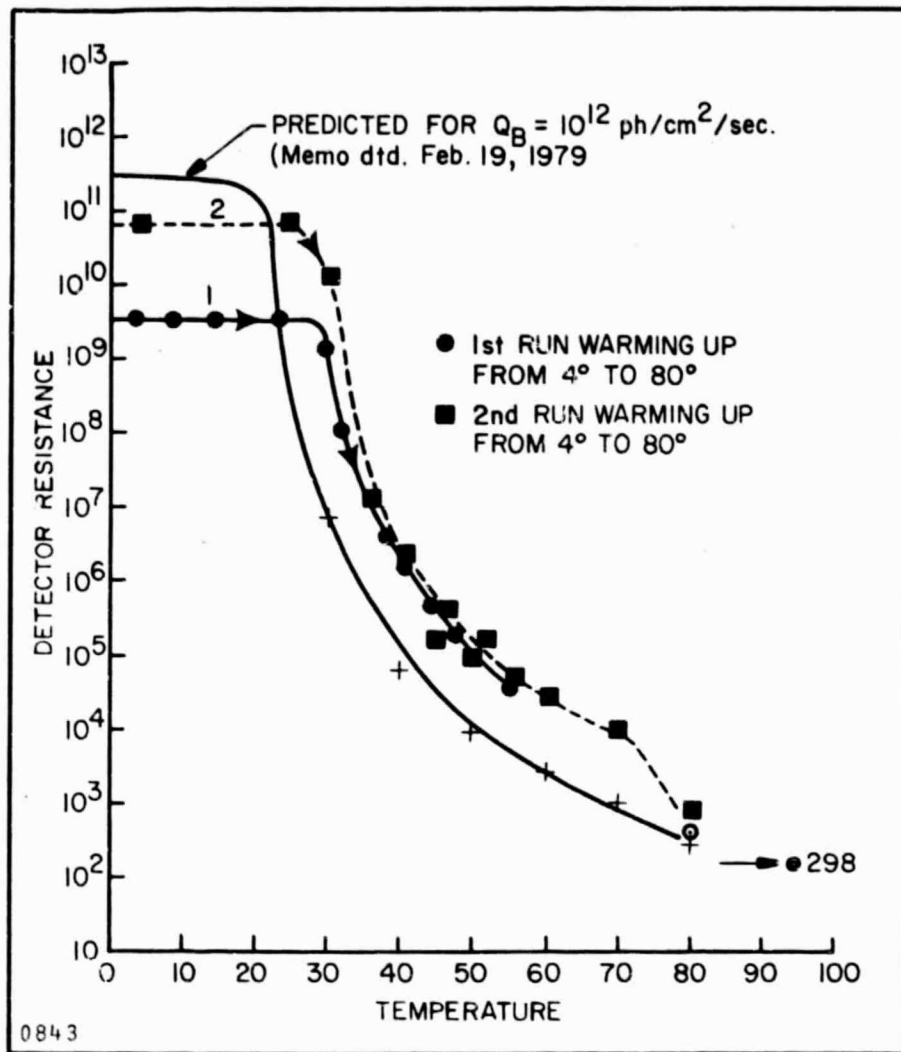
PREDICTED FOR $Q_B = 10^{12}$ ph/cm^2/sec.
(Memo dtd. Feb. 19, 1979

DETECTOR RESISTANCE

10^{13}
10^{12}
10^{11}
10^{10}
10^9
10^8
10^7
10^6
10^5
10^4
10^3
10^2
10

2

1

● 1st RUN WARMING UP
FROM 4° TO 80°

■ 2nd RUN WARMING UP
FROM 4° TO 80°

●298

0   10   20   30   40   50   60   70   80   90   100
TEMPERATURE

0843

Figure 1. NASA Ames Detector Tests, 32-Channel CMOS MUX Worked over Range
(tied thru 1 x 10^{12} Ω load resistor to slightly different bias)
10 x 10 x 40 mil Al contacted detector

3.0   MODULE FABRICATION

The steps involved in fabricating the demonstration modules are

listed below.

1. Apply ion implanted ohmic contacts on both sides of a .25 mm

    thick Si:Ga wafer

2. Activate ion implant

3. Chrome-gold metallize both sides of wafer

- 2 -

4. Slice Si:Ga into 1.02 mm wide strips

5. Etch to remove sawing damage to slices

6. Glue Si:Ga strip to the edge of metallized .25 mm ceramic substrates

7. Apply conductive epoxy bead to the interface between the substrate and detector strip

8. Mount detector assembly on sawing fixture

9. Cut slots and remove from fixture

10. Etch to remove surface damage

11. Mount to hybrid substrate

12. Epoxy attach resistors and electronics chips

13. Wire bond electronics to hybrid substrate

14. Place hybrid substrate into test fixture with indium foil thermal interface

15. Weld wires to fixture feed-throughs

16. Attach cap

Details of these processing steps have been presented in the Monthly Status Reports.

Two types of modules have been produced for this program. Two modules contain Siliconix M107 enhancement mode, p-channel MOSFET amplifier chips, and a third module contains a Carson Alexiou 32-channel CMOS multiplexer with one channel wired to a detector.

4.0   DIODE CALIBRATION

In preparation for testing the modules, the temperature diodes included with the modules were calibrated with the NASA-supplied calibrated temperature diode. The calibration results are shown in Figure 2 for the module diode used with the circuit shown in Figure 3.

- 3 -
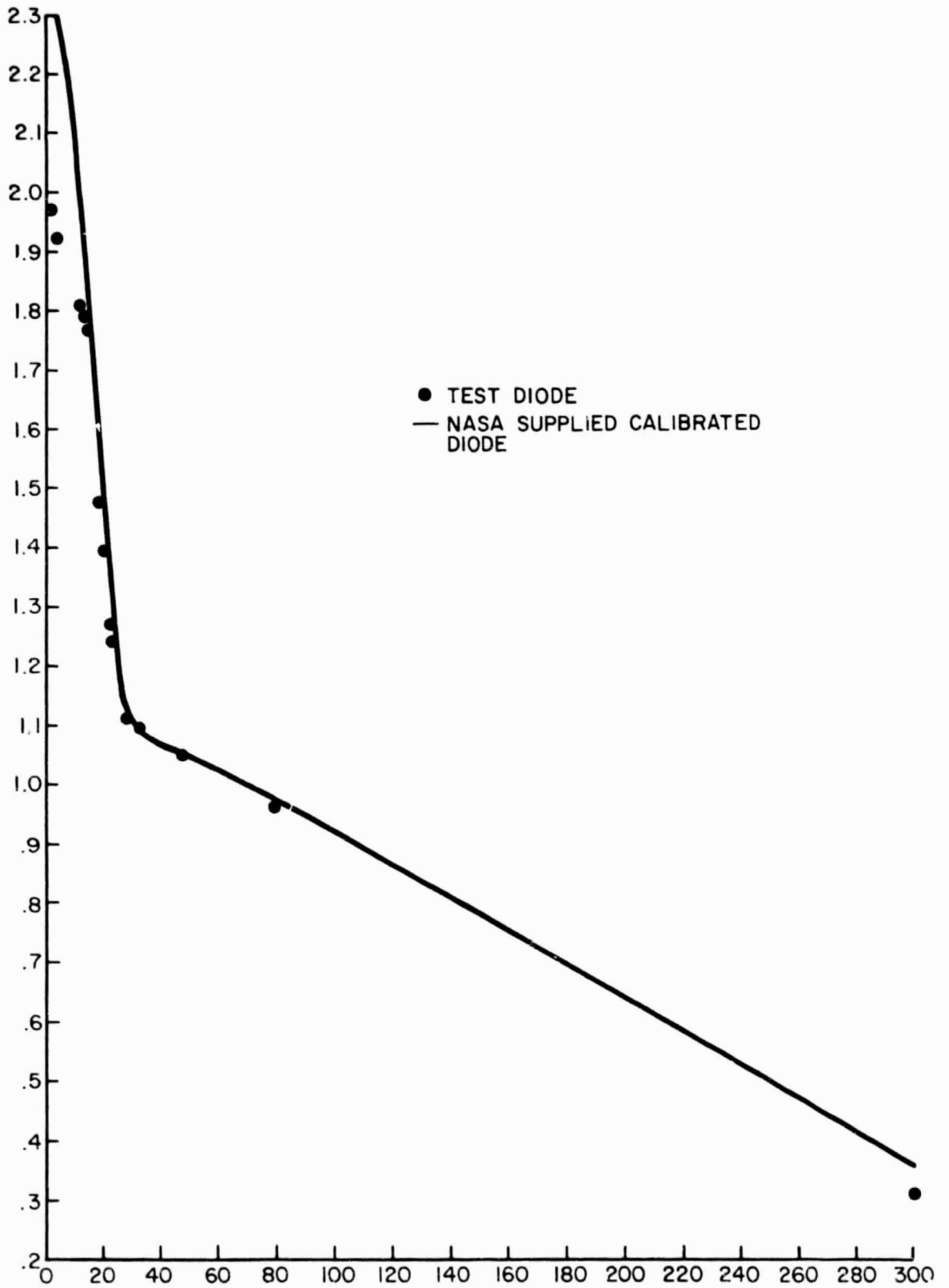
0844   Figure 2.   Temperature Diode Calibration
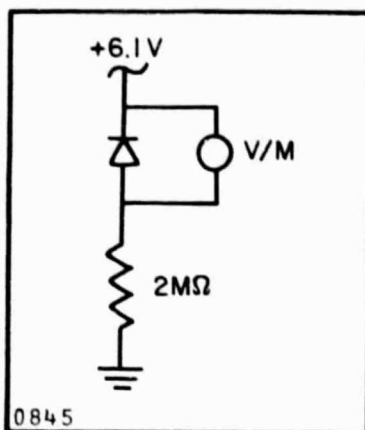
- 4 -

Figure 3. Temperature Sense Diode

5.0 SINGLE CHANNEL MODULE

The two single channel modules #1 and #3 contain Siliconix M107 CMOS devices.

5.1 Module #3

The schematic for module #3 with the M107 preamp is shown in Figure 4. On this module three load resistors are mounted such that for any test a 1×10^{10}, 1×10^{11} or 1×10^{12} Ω load resistor may be selected. Initially the M107 was tested warm with the 1×10^{12} Ω load resistor. However, the device failed to bias on correctly due probably to leakage currents. Next the 1×10^{11} Ω load resistor was tried. This resulted in marginal performance. The M107 could be biased on but control of the drain current was limited. Also the time constants involved were very long. This situation may or may not have improved with cryogenic operation. However, the decision was made to use the 1×10^{10} Ω load resistor because of the guaranteed correct bias control. The load resistance increased to 3×10^{10} cold. The noise was measured warm with the detector lead open. The results are shown in Figure 5. Low noise operation was indicated. The gain measurements both warm and cold ($2°K$) are shown in Figure 6. The initial test of the background was quite large

- 5 -

Figure 4. NASA Ames - Module #3
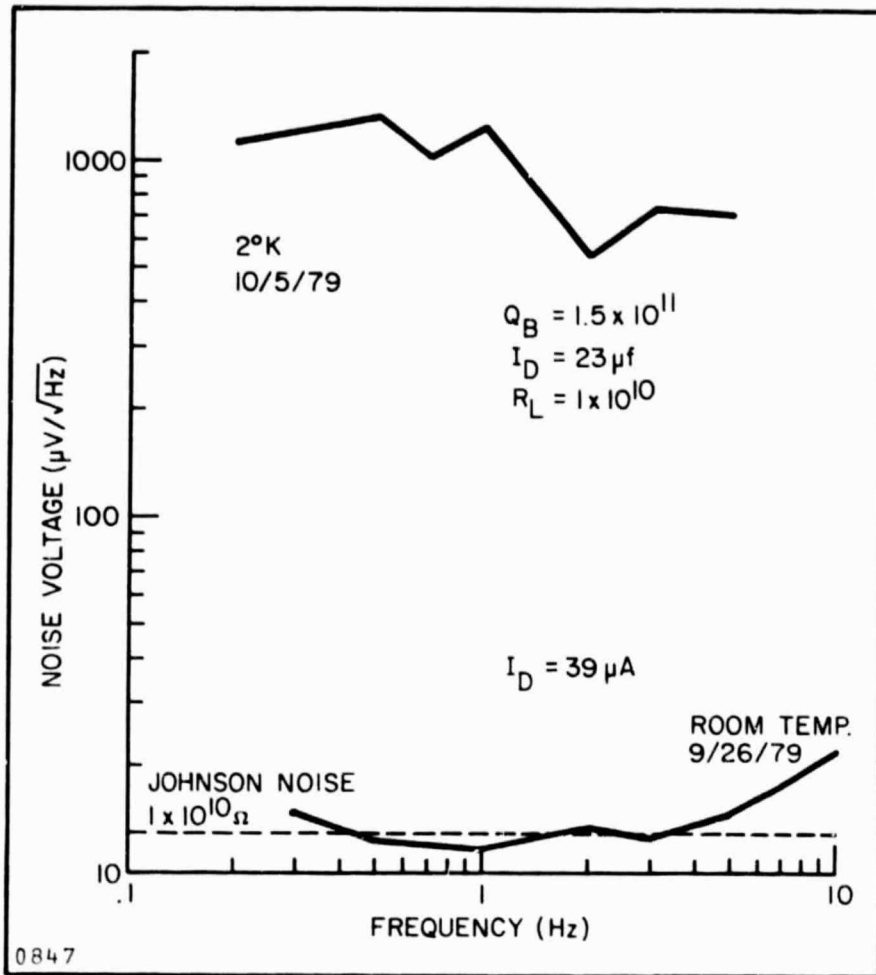

CRACK DOES
NOT AFFECT
CONTINUITY

- 6 -

0846
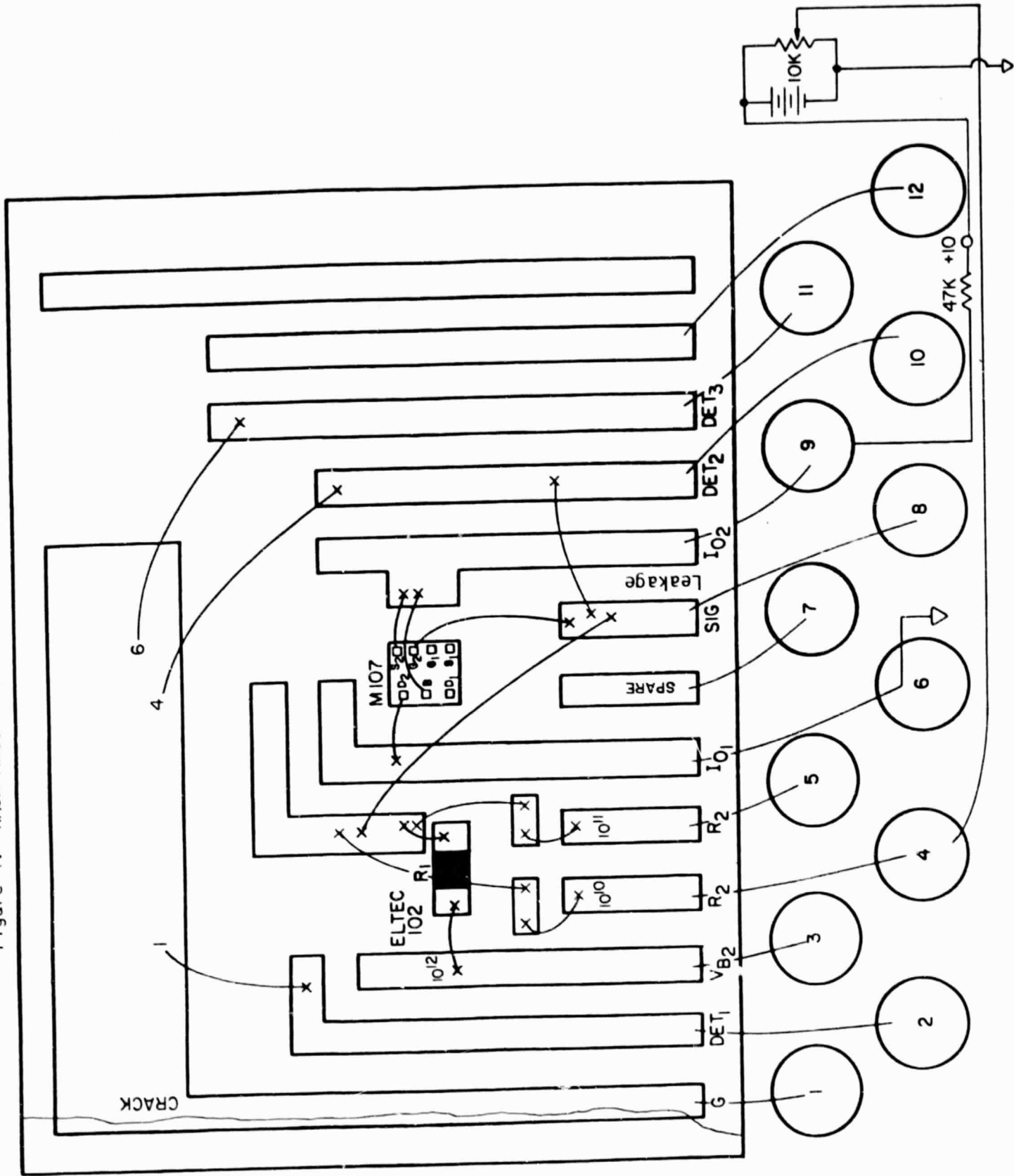
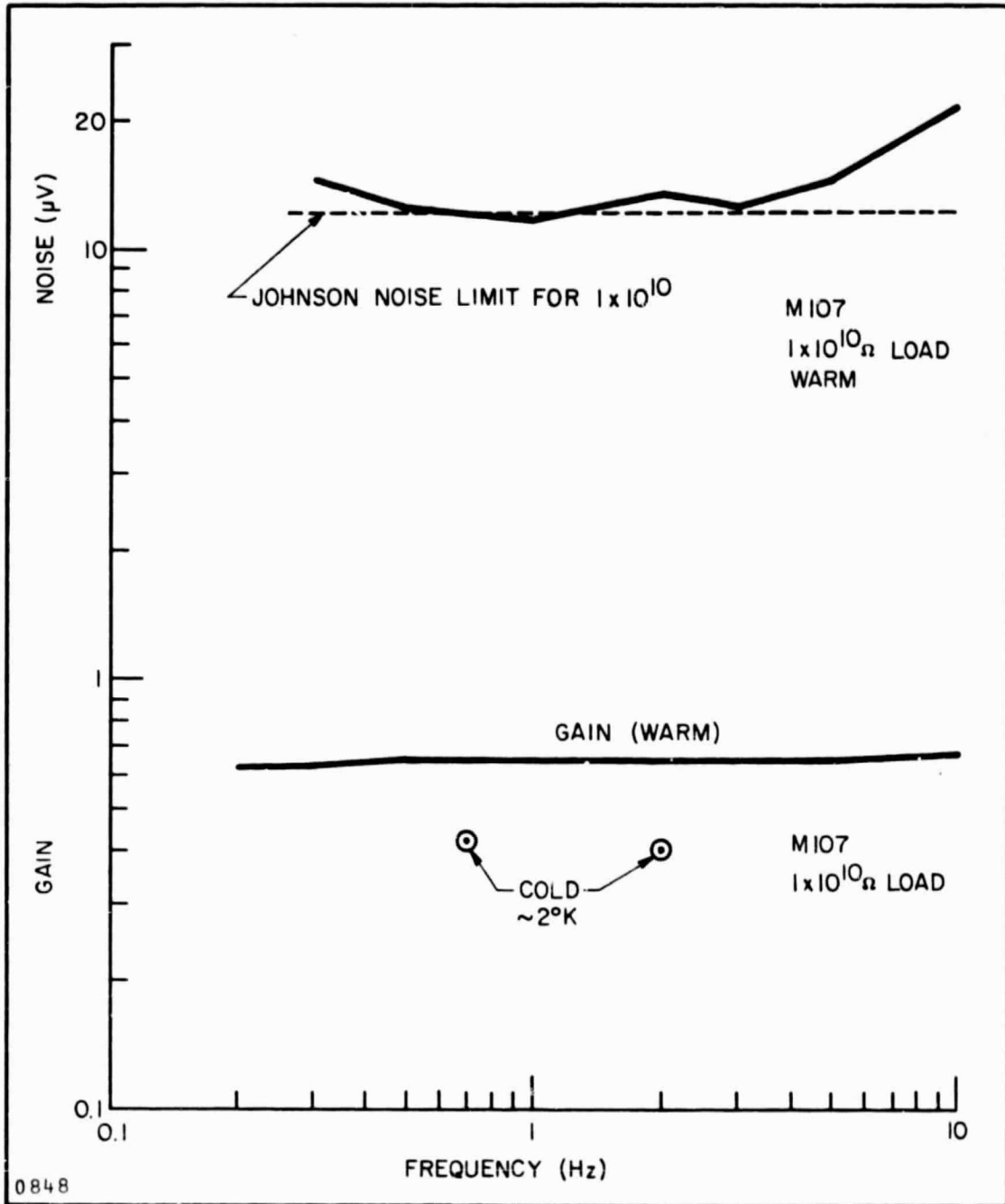Figure 5. M107 #3 CMOS Preamp, Noise vs. Frequency

Figure 6. M107 #3 Module Gain

(3 x 10^{13} photons/cm^2/sec.). The detector resistance, therefore, was assumed to be smaller than 1 x 10^{10} Ω. The signal response from a chopped blackbody was measured to be 200 μvolts. In the second test the background was reduced to ~ 1.5 x 10^{11} photons/cm^2/sec. and nearly two orders of magnitude increase in signal voltage response was observed as shown in Figure 7. During this test the noise voltage was also measured and shown in Figure 5. The
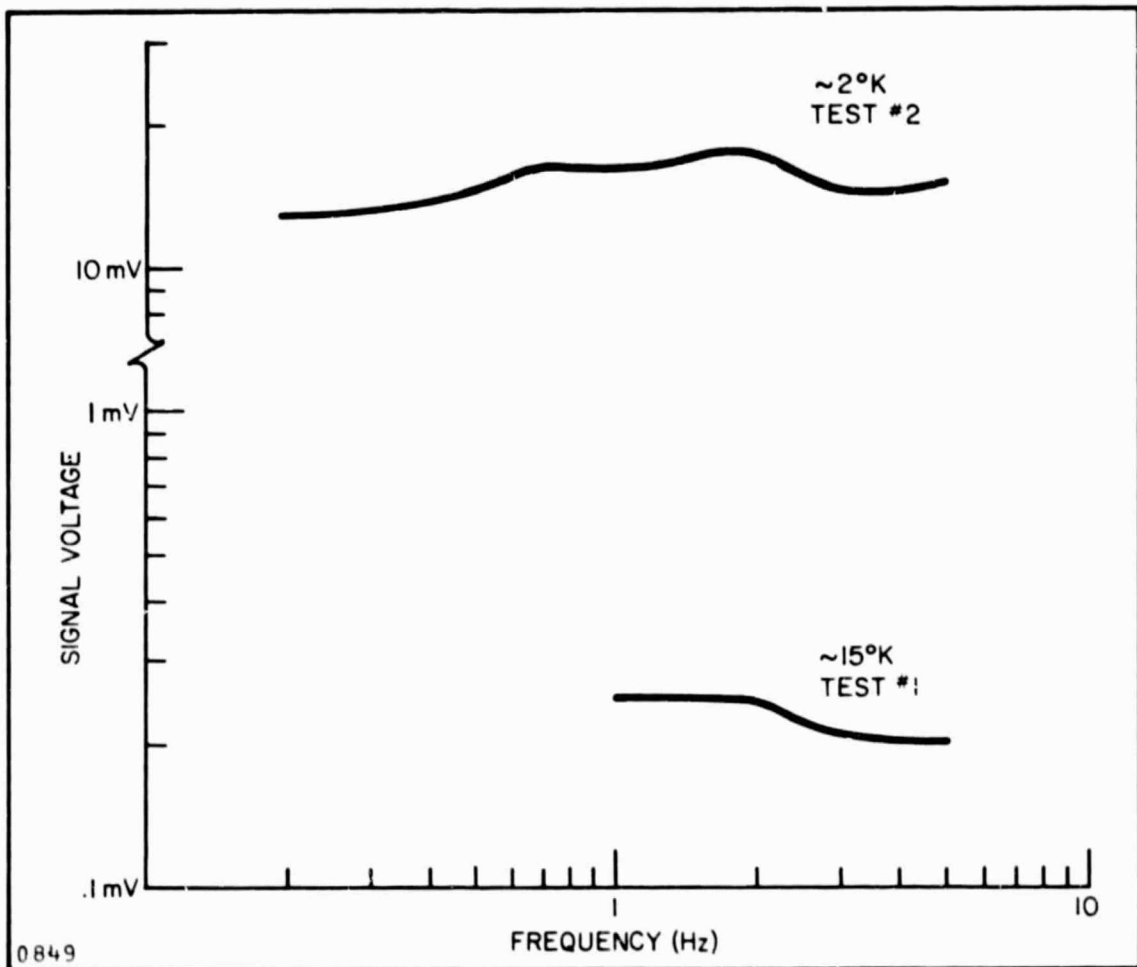

Figure 7. Signal Output Voltages

noise was quite high varying about 1 mV/$\sqrt{\text{Hz}}$. This is substantially larger than the Johnson noise of the detector load resistor combination or generation recombination noise and is additional detector noise. The detector bias was 7 volts and the detector resistance (cold) was 1.5 x 10^{10} Ω.

5.2   Interpretation of the Results of the Tests of Module #3

When detector performance is BLIP, quantum efficiency and photo-conductive gain can be calculated from the relationship

$$\frac{N_{gr}}{R} = \frac{2 \not{A} \, \not{G}_{pc} \, \sqrt{\eta \, Q \, A}}{\not{A} \, \eta \, \not{G}_{pc} \, \lambda/hc}$$

since G_{pc} cancels. However, analysis using this method yields a very low quantum efficiency and an unreasonably high photoconductive gain. The correct interpretation is that there is excess noise and the detectors are not BLIP.

The analysis approach used was to calculate photoconductive gain from the detector bias voltage and assumed lifetime and mobility.

$\therefore$ Assuming $\tau = 1.3 \times 10^{-9}$ sec.

$\mu = 1 \times 10^4$ cm^2/Vsec.

$G_{pc} = \tau \, \mu \, E/L = (1.3 \times 10^{-9})(1 \times 10^4)(276)/.0254$

Where E = bias volts/cm = 7/.0254 cm = 276

L = .0254 cm

$$\boxed{\therefore G_{pc} = .14}$$

Using this value of G_{pc}, η can be calculated from responsivity.

Measured Responsivity

$$\boxed{R = 15 \text{ mV/1} \times 10^{10}/7.42 \times 10^{-11} \text{ W} = .02 \text{ amps/W}}$$

Theoretical Responsivity

$$R = q \, \eta \, \lambda \, G_{pc}/hc \text{ amps/W}$$

$$\boxed{R = 3.542 \, G_{pc} \, \eta \text{ amps/W}}$$

$$\therefore \text{ If } G_{pc} = .14$$

$$\text{Then } \eta = \frac{.02}{(3.542)(.14)}$$

$$\boxed{\eta = 4\%}$$

Theoretical G-R noise voltage

$$N_{g-r} = 2 q G_{pc} \sqrt{\eta Q_B A} R_{eq}$$

$$= 2 (1.602 \times 10^{-19})(.14)\sqrt{(.04)(1.5 \times 10^{11})(5 \times 10^{-4} \text{ cm}^2)} \, 1 \times 10^{10}$$

$$\boxed{N_{g-r} = .78 \ \mu V/\sqrt{Hz}}$$

Measured noise voltage

$$\boxed{N_{meas} = 1000 \ \mu V/\sqrt{Hz}}$$

5.3   Conclusion

The quantum efficiency is 4% and the noise is three orders of magnitude high.

6.0   32-CHANNEL CMOS MULTIPLEXER TESTS

6.1   Module #2

This module as shipped to NASA Ames contains two CMOS multiplexers, two resistors, and approximately 10 detectors (see Figure 8). Two resistors were connected in parallel at $1 \times 10^{12} \ \Omega$ and at $1 \times 10^{10} \ \Omega$ under the premise that after the tests were performed at high background in which the detectors were expected to be $1 \times 10^{10} \ \Omega$ the small resistor could be cut out leaving the $1 \times 10^{12} \ \Omega$ resistor for the low background test. The high background tests were performed at approximately 3×10^{13} photons/cm²/sec. One detector was connected to one input of the CMOS multiplexer (CMOS Channel #13). The

Figure 8. NASA Ames - Module #2

32 Channel Simulation

0850
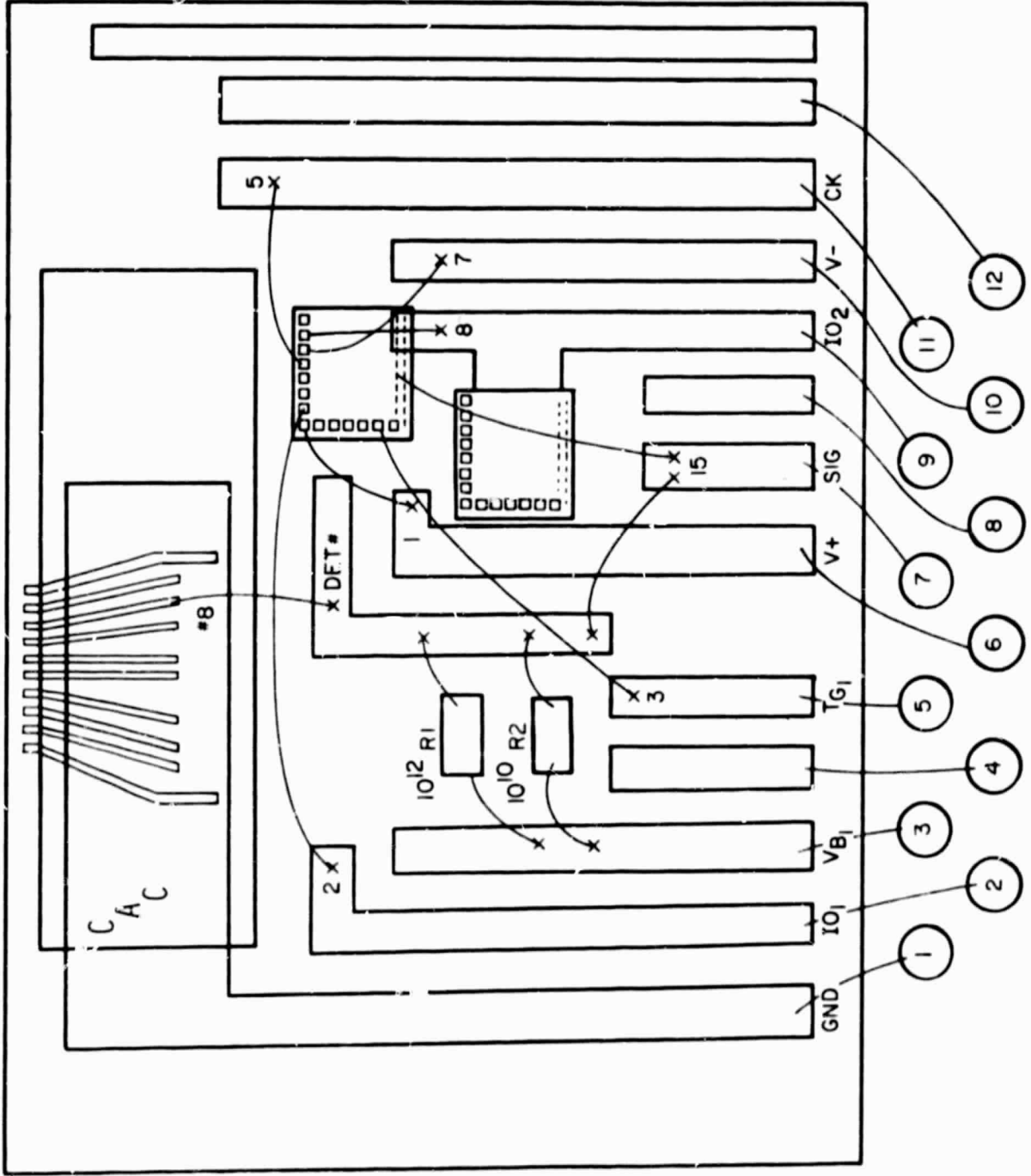
detector lead was left open for the initial warm noise tests because of the detectors low impedance at room temperature (~ 50Ω). Channel #13 was measured both dynamically (2.5 KHz clock rate) and statically (unclocked). Upon the initial cool-down Channel #13 apparently suffered static damage. The detector input was disconnected from Channel #13 and reconnected to Channel #9. Static and dynamic tests were performed warm. The results are shown in Figure 9. The Johnson noise of the warm load resistor is approximately 12.8 μV $\sqrt{Hz}$.
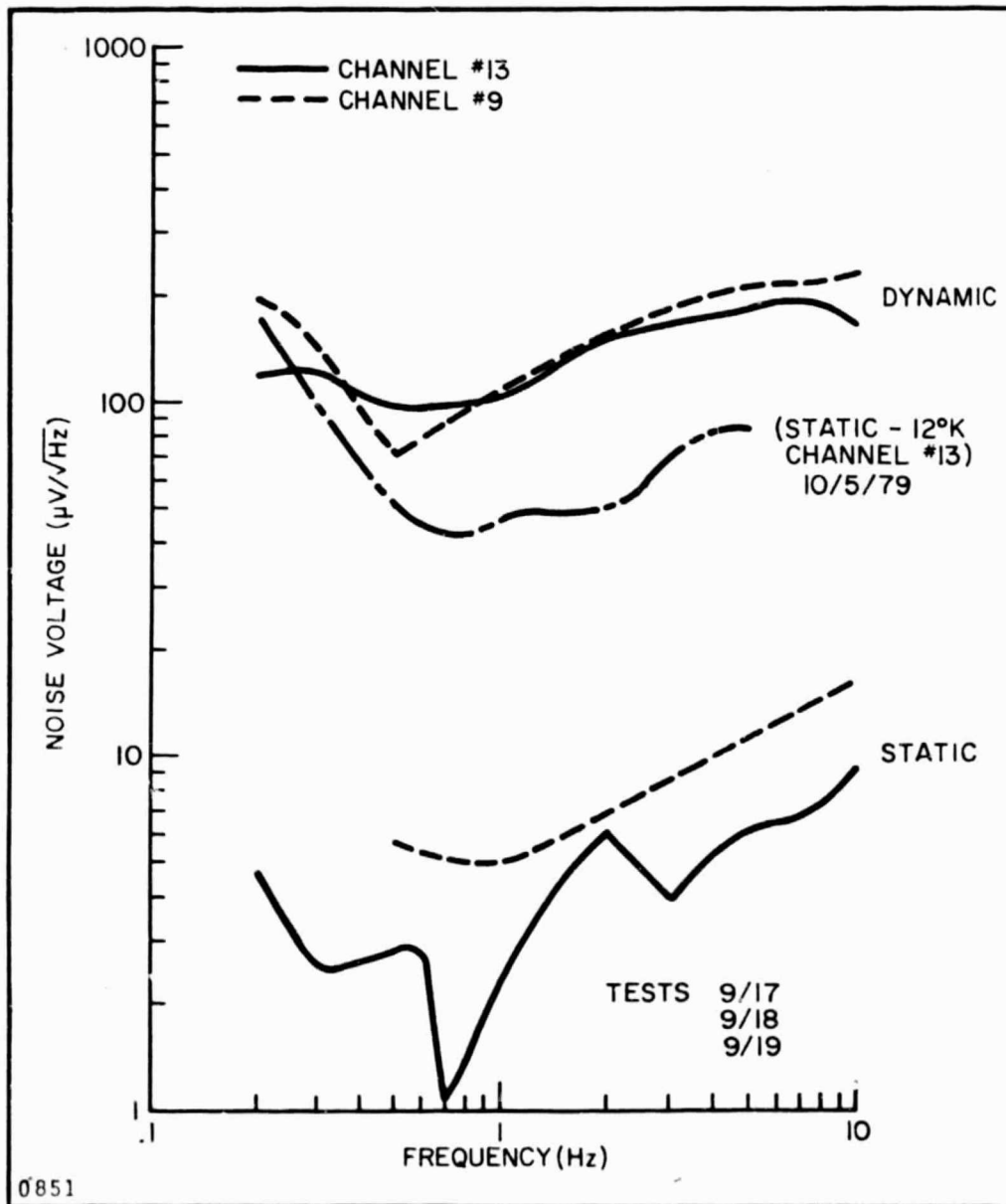

Figure 9. CMOS Multiplexer, Noise vs. Frequency

The dynamic warm noise tests resulted in noise values around 150 $\mu V/\sqrt{Hz}$. The gain of the multiplexer was not measured on this program unfortunately, however, it should lie between .7 and .8. Therefore, the gain corrected warm noise appears to be in the vicinity of 200 $\mu V/\sqrt{Hz}$ or 16 times Johnson noise. The results of the static tests indicate noise levels of 4 $\mu V/\sqrt{Hz}$ which is below theoretical Johnson niose because of low gain of the CMOS multiplexer.

The normal waveforms of the CMOS multiplexer are shown in Figure 10. The "fixed pattern noise in Figure 10a is large due to the fact that 31 inputs of the CMOS are left open and only one is tied to a bias (detector and load resistor bias). In normal operation the active channel is biased to 0V thus allowing sufficient dynamic range both positive and negative. In Figure 10b the scope intensity is increased to highlight the switching spikes during dynamic operation. At 2.5 KHz the switching spikes contribute significant noise as seen in Figure 9. These spikes, however, do settle out quite fast as seen in the expanded time scale of the CMOS waveform in Figure 11a. The exact dependence of noise and gain on clock rate is unknown and should be investigated further. Also the measured noise should vary as a function of where the CMOS output is sampled in time; the closer to a switching spike, the noisier the results, obviously.

During rework of the module (Channel #13 to Channel #9 switch) additional degradation to the multiplexer occurred. This degradation appears as additional clock noise as seen in Fiure 11b. Due to this degradation an additional CMOS multiplexer was attached to the module. Again Channel #13 was selected to be the active input channel (selected at random).
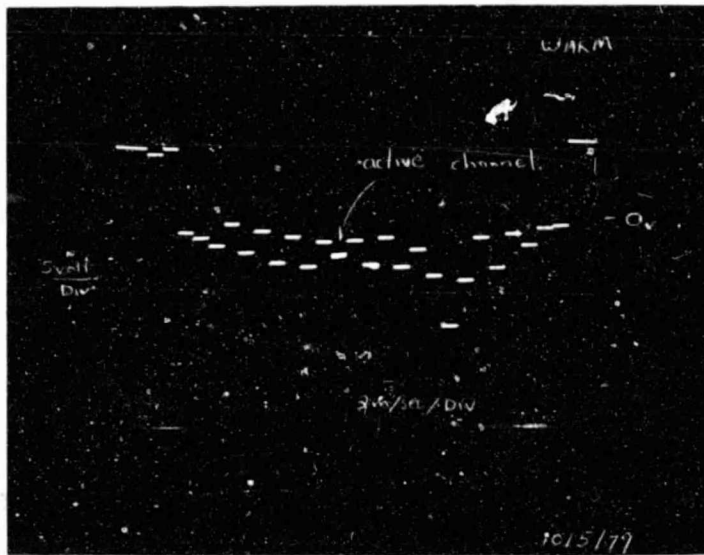
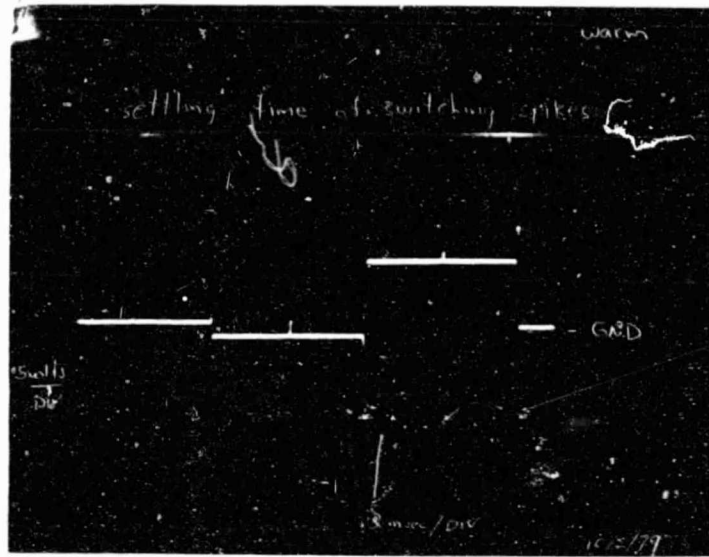(10a)

Normal Output Waveform of CMOS MUX at Room Temperature
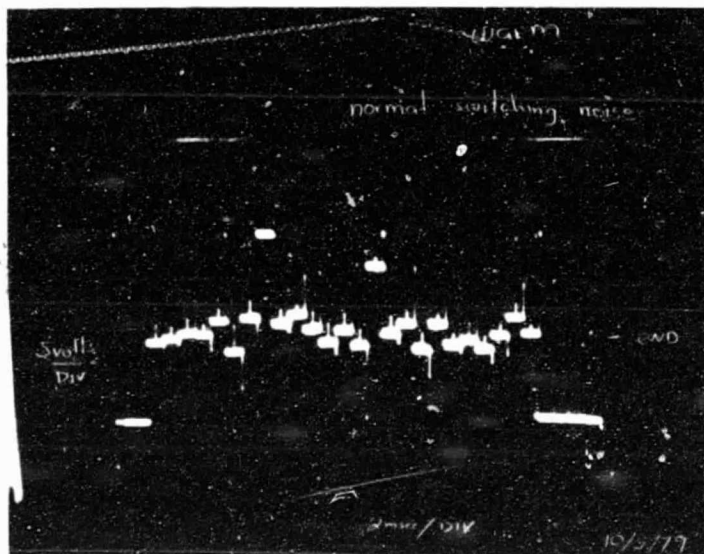
(10b)

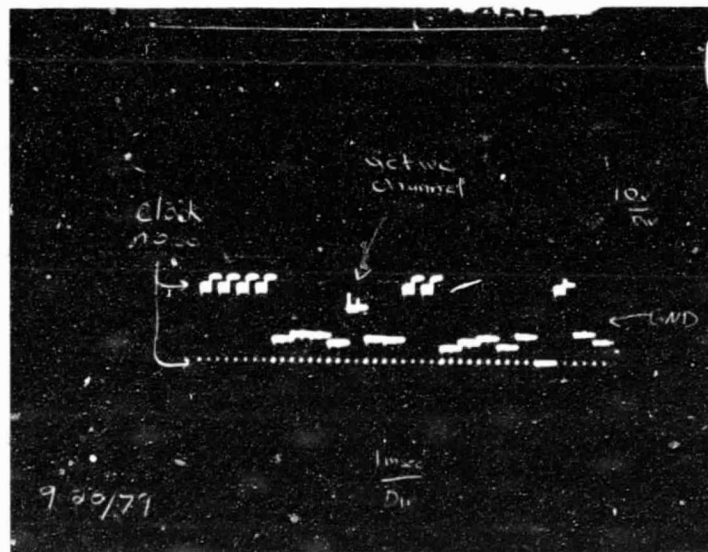Intensity Enhanced to Show Switching Noise of CMOS MUX - Room Temperature

Figure 10.   CMOS MUX Waveforms

- 15 -

(11a)

Expanded Time Scale to Show Settling Time of Normal CMOS MUX Switching
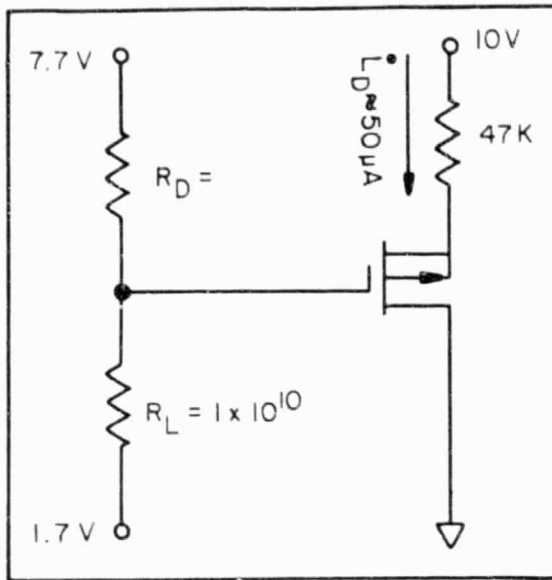Spikes - Room Temperature

(11b)

Abnormal Switching Noise of CMOS MUX Channel #9 Active - Room Temperature

Figure 11.   CMOS Multiplexer Waveforms

7.7 V

$R_D =$

$L_D \approx 50 \mu A$

10 V

47 K

$R_L = 1 \times 10^{10}$

1.7 V

0856

Figure 12.   CMOS MUX Bias

This device was cooled for noise measurements at a more moderate background, $\sim 1.5 \times 10^{11}$ photons/cm^2/sec. The bias circuit, voltages, and currents used at 12°K for the CMOS operation are shown in Figure 12. The bias circuit points out that the detector resistance in this case is very poor ($< 1 \times 10^9$) because the gate of the CMOS input appears to be at about 7.7 volts. Thus there is not bias across the detector and no photo gain. The poor detector performance was verified in that the detector would only respond slightly to a soldering iron. The statis noise measurements from this test are also shown in Figure 9. With the detector in the circuit and at 12°K the noise voltage appears to be approximately 1 order of magnitude larger than previous static tests.

The dynamic waveform of the multiplexer also changes slightly at this temperature. A photograph of the output waveform is shown in Figure 13. As can be seen the output levels are now at a slope as if the rise time associated with each level has increased significantly. This effect is first noticed around 15°K.

6.2   Interpretation of Module #2 Tests (also see Section 5.2)

Photoconductive gain for bias voltage = 2V

$$G_{pc} = (1.3 \times 10^{10})(1 \times 10^4)(78.7)/.0254 = .004$$

Assume lifetime is an order of magnitude shorter than normal yielding low resistance.

- 17 -

GND
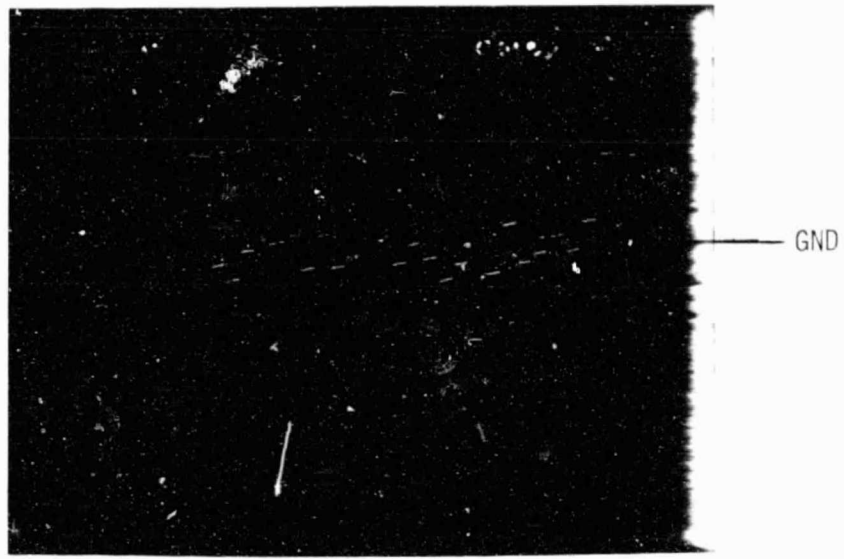
0857

Figure 13.   MUX Waveforms at 2°K

Assume η = 4%

Measured Noise

$$N_{meas} = 60 \ \mu V$$

Theoretical Background Noise Voltage

$$N_{gr} = 2 \ (1.602 \times 10^{-19})(.004) \ \sqrt{.04 \ 1.5 \times 10^{11} \quad 5 \times 10^{-4} \quad 1 \times 10^{9}}$$

$$= 2.2 \ nV/\sqrt{Hz}$$

Theoretical Johnson Noise Voltage

$$N_{Johnson} = \sqrt{4KTR} = .80 \ \mu V/\sqrt{Hz}$$

6.3   Conclusion

The theoretical Johnson noise is much larger than generation recombination noise. However, electronics noise is larger than either type of detector noise.

- 18 -

7.0   M107 SINGLE CHANNEL PREAMP

7.1   Module #1

This module is untested, however, the CMOS chip has been cleaned since it was discovered that dust particles had settled on the chip. The CMOS preamps were received from the manufacturer in this condition, therefore it is hoped that the cleaning will improve the input impedance and allow load resistors in the 1×10^{11} to 1×10^{12} Ω range. A schematic of Module #1 is shown in Figure 14.

8.0   CONCLUSION

Responsivity and D* have been calculated for the M107 Module #3 tests according to the formulas listed in Figure 15.

At 2°K the load resistor was assumed to be the limiting impedance (detector higher impedance) at 1×10^{10} Ω. Responsivity is calculated to be in the range of 34 ma/watt to 60 ma/watt as shown in Figure 16. The corresponding D* is in the range between 2×10^{10} and 5×10^{10} cm $\sqrt{Hz}$/watt. The D* BLIP for this experiment is approximately 2×10^{13} cm $\sqrt{Hz}$/watt, or 3 orders of magnitude greater than measured (assuming a quantum efficiency of .5). The theoretical D* associated with the Johnson noise from a 3×10^{10} Ω load resistor is

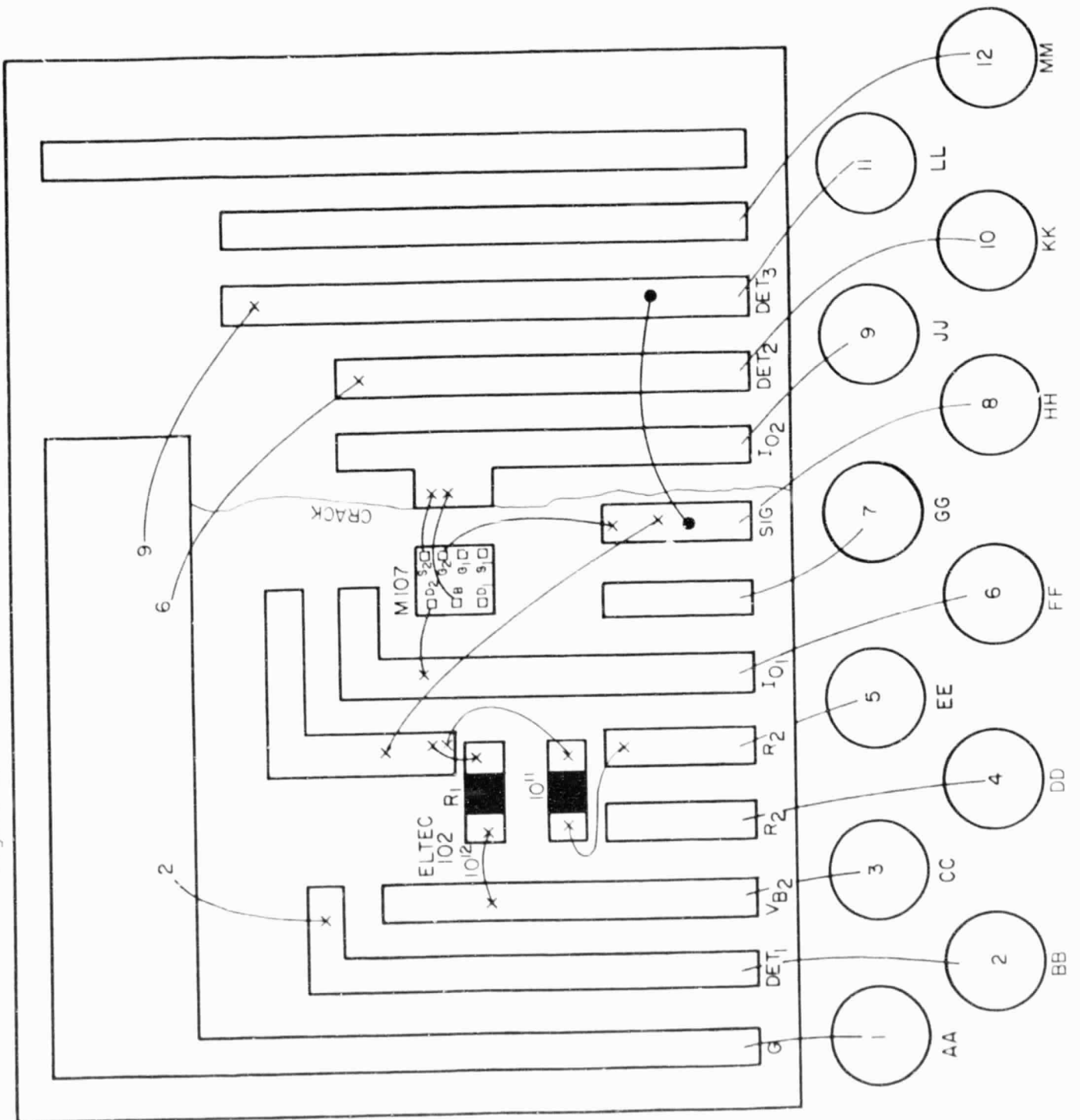$$D^* = \frac{R_{esp} \sqrt{A_d} \, \Delta f}{I_n} = 6.54 \times 10^{14} \text{ cm } \sqrt{Hz}/\text{watt}$$

$$R_{esp} = \frac{\eta \, q \, \lambda}{hc} = 1.77 \, \frac{amp}{watt} \text{ theoretical responsivity}$$

$$I_n = \sqrt{\frac{4 \, KT}{R}} = 6.1 \times 10^{-17} \text{ amps theoretical noise}$$

$$A_d = 5 \times 10^{-4} \text{ cm}^2$$

$$\Delta f = 1 \text{ Hz}$$

Figure 14. NASA Ames - Module #1

CRACK DOES
NOT AFFECT
CONTINUITY

0858

Figure 15. Equations for D* and Responsivity

Power on the detector from blackbody

$$P_D = \frac{H(\Delta\lambda)(D_{bb})^2 \, (A_d)(\tau_w)(\tau_f) \, K}{4 \, R^2} = 7.42 \times 10^{-11} \, W$$

$H(\Delta\lambda)$ = integral of Plank's equation from $\lambda_1 = 4.35$ to $\lambda_2 = 4.42$, .005W/cm^2

(D_{bb}) = diameter of limiting aperture (blackbody), .2 cm

(A_d) = area of the detector, 5×10^{-4} cm^2

(τ_w) = window transmission, .8

(τ_f) = filter transmission, .4

K = square wave to sine wave, .45

R = range, 23.1 cm

Responsivity

$$R_{esp} = \frac{V_{sig}}{R_L \, P_D}$$

V_{sig} = measured signal divided by the gain of the cold preamp and

by the gain of measurement device

R_L = parallel combination of detector and load resistor

P_D = power on the detector

D* Calculation

$$D\star = \frac{R_{esp} \, \sqrt{A_d}}{V_{noise}/R_L}$$

V_{noise} = Voltage noise measured divided by the square root of the

bandwidth, the cold preamp gain and the measurement device
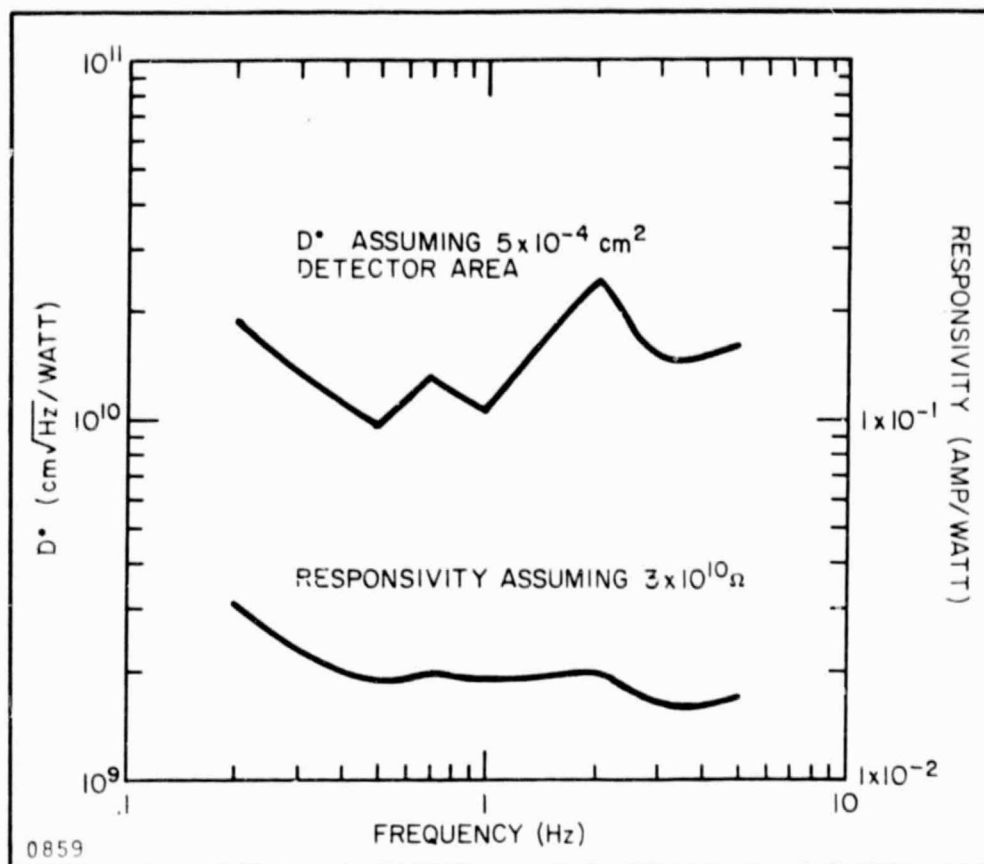
gain

- 21 -

Figure 16.   M107 #3 Radiometric Test

It appears that this detector is an order of magnitude low on responsivity
and more than 3 orders of magnitude high in noise.

9.0   SUGGESTED DETECTOR IMPROVEMENTS

The detector material should be analyzed using Hall techniques before
detailed doping improvements could be suggested.